Current Research (1989) Newfoundland Department of Mines, Geological Survey of Newfoundland, Report 89-1, pages 63-79

SEDIMENTOLOGICAL STUDIES IN THE EASTPORT BASIN: NOTES ON THE PETROGRAPHY OF THE LATE PRECAMBRIAN CONNECTING POINT GROUP AND PROVENANCE IMPLICATIONS

Tomasz Dec, Ian Knight and Sean J. O'Brien
Newfoundland Mapping Section

ABSTRACT

The sedimentary rocks of the Connecting Point Group are volcaniclastic lithic arenites, and are compositionally similiar to the pyroclastic rocks of the upper part of the underlying Love Cove Group. The lower 1500 m of the succession consists of felsic volcanic and metamorphic detritus and a subordinate andesitic component. Andesitic clasts represent the dominant lithic component of sandstones, beginning at a pebbly mudstone (mixtite) and continuing upward for over 1500 m. However, in this upper interval, the fine-grained tuffs, and the matrix and blocks of tuff within the mixtite, suggest that felsic volcanism was continuous, and that only the proportion of andesitic to felsic volcanism changed at this stratigraphic level.

The petrographic data suggest that the source terrain of the volcaniclastic sediments was a mature island-arc complex, developed on a continental crust and/or island-arc crust that included medium- to high-grade metamorphic rocks.

The ratio of quartz to pyroclastic detritus, which is indicative of sediment maturity, declines upward. This is interpreted to reflect, 1) the widening of the rifted arc basin so that narrow, shallow-water zones of sediment reworking were isolated from the zones of sediment remobilisation on the volcaniclastic apron, and 2) the large volume of pyroclastic material generated in the arc, overwhelmed the depositional basin, and caused slope instability and rapid sediment remobilisation. An episode of basin extension, previously correlated with the formation of mixtite and intrusion of mafic dykes and plutons, appears to coincide with the increase in the proportion of andesitic detritus in the sediments of the upper part of the Connnecting Point Group.

INTRODUCTION

The late Precambrian Connecting Point Group is a marine, volcaniclastic sequence at least 3500 m thick (Hayes, 1948). Preliminary lithostratigraphical and sedimentological surveys by Knight and O'Brien (1988), indicate that the lower 2400 m are the product of sedimentation in a system of submarine aprons, adjacent to a volcanic arc. The volcanic arc is considered to be represented by the Love Cove Group, equivalent age volcanic sequences and related plutons that lie west of the western Avalon Zone.

There are two major objectives of this petrographic study: 1) to determine the provenance of the detritus in the upper Love Cove and Connecting Point groups, and thus advance our understanding of the geotectonic setting of its sedimentation, and, 2) to evaluate aspects of emplacement of the volcaniclastic sediments, such as the deposits of gravity-driven sediment flows.

The diagenesis, metamorphism and deformation of the discussed sediment deposits have not been examined in detail. The sediments have been regionally metamorphosed to a greenschist facies. Deformation and accompanying metamorphism affect the sequence most severely in the vertical to inverted, eastward-facing limb of the Willis Reach syncline (Figure 1), where there is substantial bedding-parallel flattening of the strata. This affects the rocks principally in the Long Reach–Pretty Island and Hail Island–Coal Island sections. Gently folded and dipping strata, east of the area around Eastport and Salvage, are almost pristine in their preservation of volcanic textures.

STRATIGRAPHY AND LITHOFACIES

Pyroclastic rocks and epiclastic sedimentary rocks of the upper part of the Love Cove Group and the overlying Connecting Point Group, form a conformable succession in the Eastport basin (O'Brien and Knight, 1988). Shales, and fine to coarse pyroclastic rocks and minor tuffaceous turbidites, characterize the uppermost part of the Love Cove Group. An assemblage of ten lithofacies combine in different proportions to constitute the six lithostratigraphic units that make up the Connecting Point Group (Knight & O'Brien, 1988). Five of these units (C-1 to C-5) are shown in the graphic logs on Figure 2; the sixth unit (C-6) has not been logged in detail and is thus not shown on the figure.

The lower 1750 m of the Connecting Point Group form an upward-coarsening succession composed of three units.

This project is a contribution to the Canada–Newfoundland Mineral Development Agreement, 1984–1989

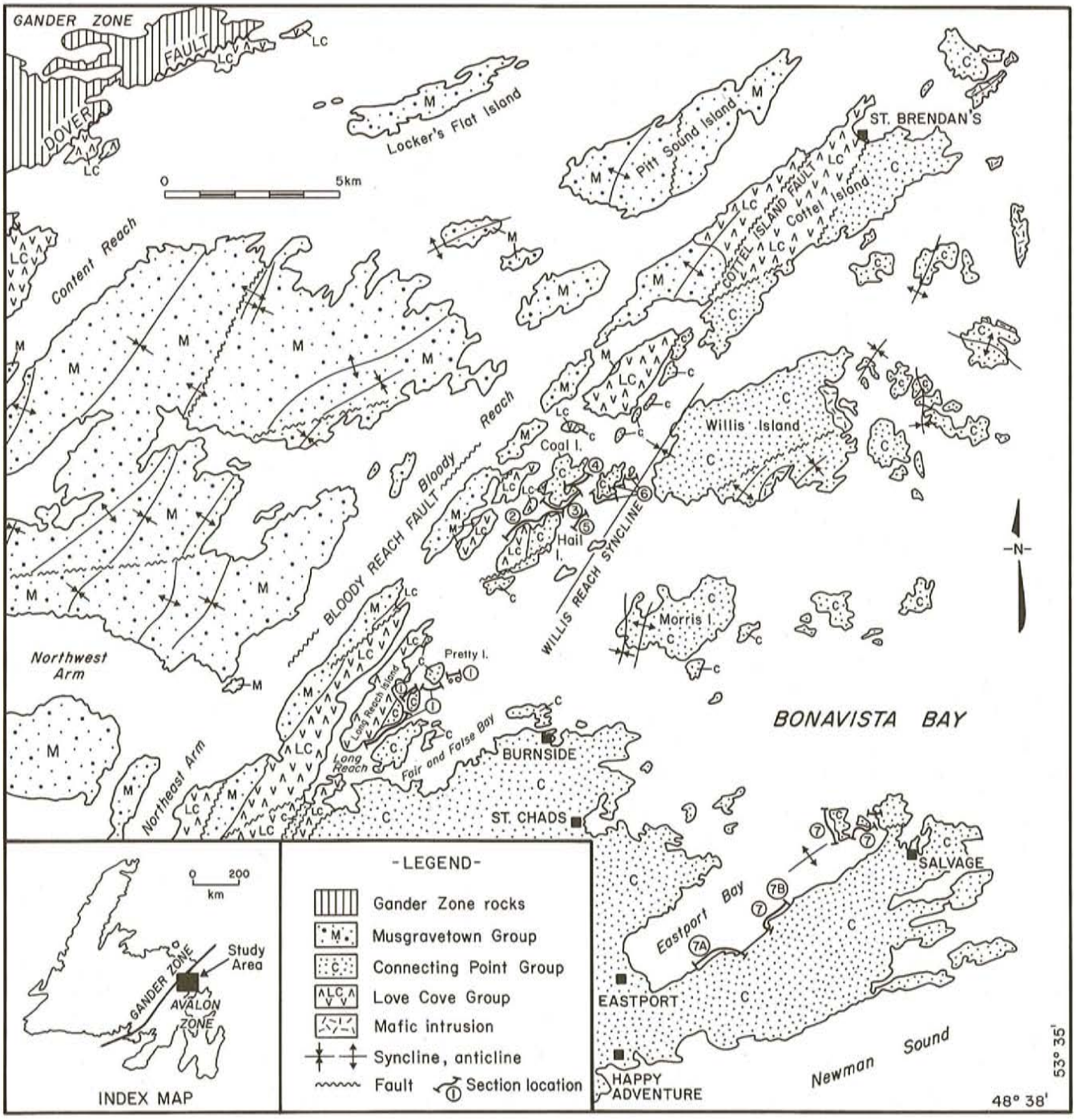

Figure 1. *Geological map of the Eastport area of Bonavista Bay showing the location of stratigraphic sections and sampling; modified from O'Brien (1987), Knight and O'Brien (1988) and O'Brien and Knight (1988).*

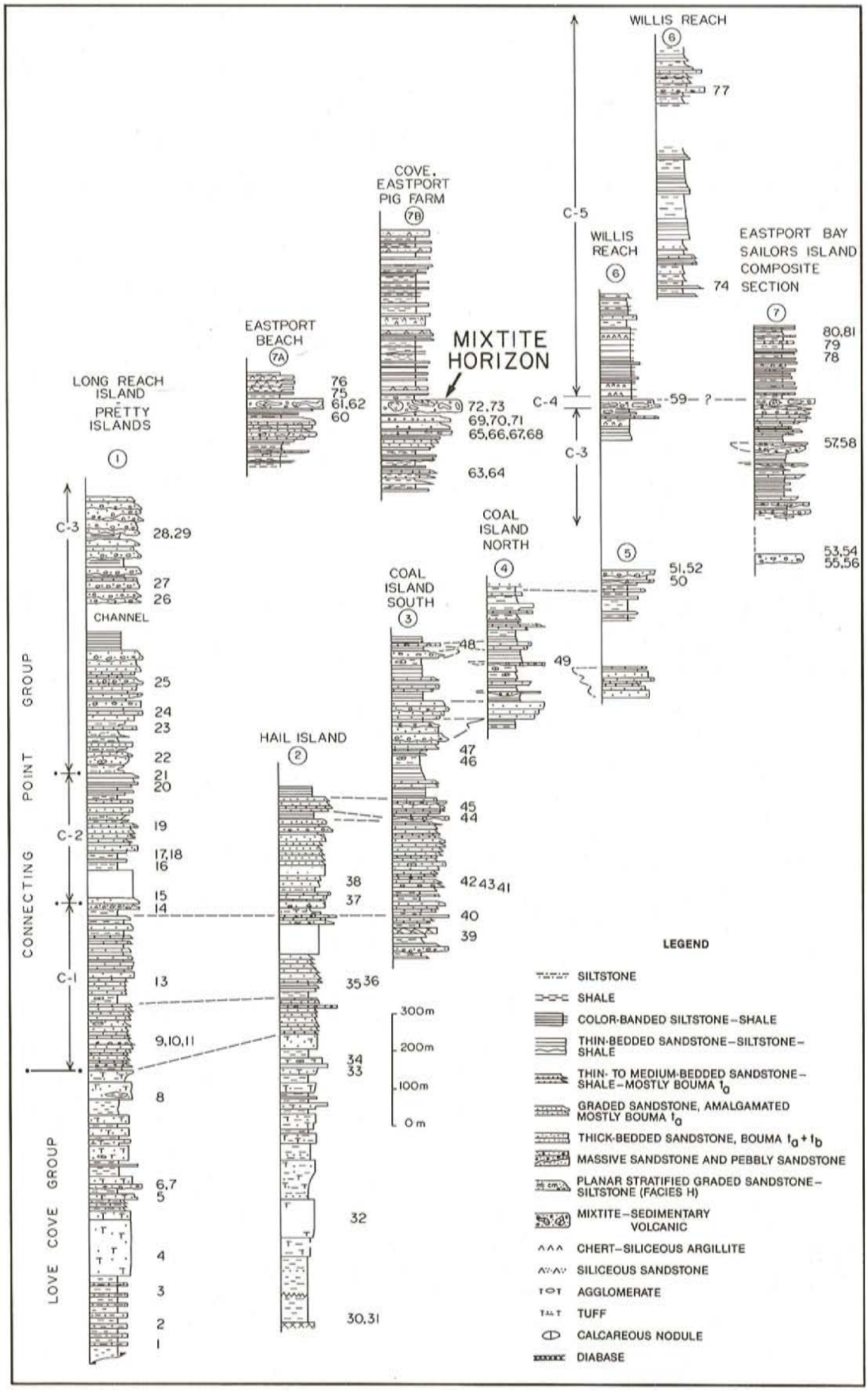

Figure 2. *Graphic logs of sections through the upper Love Cove Group and the overlying Connecting Point Group showing stratigraphic location of sample numbers; C 1 to 5 lithostratigraphic units and sedimentary logs, modified from Knight and O'Brien (1988, Figures 3 and 4).*

The basal unit (Unit C-1; Figure 2) comprises 400 m of thin-bedded, green–grey and buff, tuffaceous sandstone and siltstone, black shale and rare fine grained pyroclastic rocks and coarse-grained epiclastic conglomerate and sandstone. Thicker bedded, massive sandstones also occur, but bed-thickness or grain-size trends are not obvious in the unit. The succeeding unit (Unit C-2; Figure 2) is 370-m thick and consists of thickening- and coarsening-upward sequences of parallel-bedded, thin- to thick-bedded, graded, very fine- to very coarse-grained sandstone, rare pebbly sandstone and shale. The upper unit (Unit C-3; Figure 2) comprises 1000 m of thinly bedded and laminated sandstone, siltstone and shale, enclosing large lenticular, tens of metres thick, fining-upward bodies of massive sandstone and pebbly sandstone. Intervals of parallel-bedded turbidites and black shales also occur. A regional pebbly mudstone (mixtite) unit, 11- to 17-m thick (Unit C-4; Figure 2) lies above the third unit. It contains variably sized rip-up clasts and rafts of intrabasinal sediments, which are deformed, as well as pebbles and boulders of volcanic and plutonic origin. It is in turn overlain by a 500-m-thick shale-dominated sequence (Unit C-5; Figure 2), which is also characterized by thin sandstone and siltstone beds, cherts and slump deposits. Several thick sandstone beds having planar stratification and water escape structures occur in the unit immediately above the mixtite. The section that has been studied so far is completed by a succession (Unit C-6; not shown on Figure 2) over 1000-m thick, of thin to thick-bedded, turbiditic sandstones and shales organized in repetitive coarsening- and thickening-upward packages.

The sandstones of the Connecting Point Group have the characteristics of high-density turbidites deposited in both distal and proximal settings of the basin (Knight and O'Brien, 1988). The organization of the sediments up through the section indicates that deposition occurred in a variety of deep-water submarine fan settings, including low-efficiency fans during the earlier part of the basin's history, and as channeled fans having extensive levée complexes, as the basin matured. The accretion of a very thick sequence of thin-bedded, fine-grained sediment and local evidence of slumping and mass-flow transport, suggest the progradation of the depositional slope, prior to an important episode of basin extension. This phase of extension coincided with the deposition of the mixtite, which is a regional olistostrome, and includes an intrusion of a suite of small plutons and dykes of mafic composition. Post-extension basin development is marked by progradation of submarine fans.

PETROGRAPHY

Methodology

Eighty-one thin sections, ranging from tuff to small pebble conglomerate, were examined to determine the primary composition of the deposits and their sedimentary, textural and structural characteristics. Thirty-five samples of 300 points per thin section were counted in order to determine proportions of their detrital components. Metamorphism and deformation have modified the sedimentary and petrographic signatures of the rocks in question. This has often precluded reliable distinguishing of some detrital constituents, such as metamorphic quartz, from fragments of recrystallised felsic groundmass; it has also inhibited distinction between intrabasinal tuff clasts and fragments of aphanitic felsic groundmass.

The proportions of various lithic fragments were determined to analyse their abundance and significance. The matrix component was point counted on a separate channel and thin sections were stained in order to identify K-feldspar.

The point-counting technique followed the approach of Zuffa (1980, 1985; see also Gazzi, 1966; Dickinson, 1970; Ingersoll *et al.*, 1984). The results, combined with detailed petrographic examination of the clasts, serve as the data base for evaluation of the provenance of the Connecting Point Group. Geochemical data is presently not available to precisely classify the volcanic clasts. However, on the basis of the petrography, the volcanic clasts are subdivided into two general categories, 1) rhyolite–dacite and, 2) andesite–basalt; the latter group is represented dominantly by andesitic clasts.

Tuffs and Tuffites

Tuff and tuffite horizons in the upper 1000 m of the succession help elucidate the nature of the pyroclastic components in the sandstones described below (e.g., see samples 71 to 73 and 75; Figure 2). In the tuff beds, shards (Plate 1) and pumice fragments are typically replaced by quartz and feldspar (probably albite) (Plates 1, 3 and 6). Chlorite, calcite and prehnite less commonly replace glass. Throughout most of the succession in the western limb of the Willis Reach syncline, felsic glass is apparently rare,

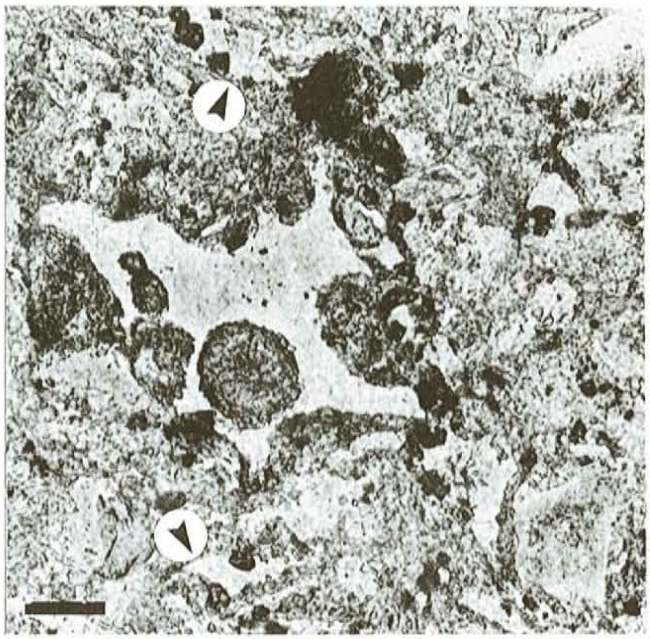

Plate 1. *Fragment of felsic pumice from a bed of crystal tuff; glass is altered to albite and chlorite and the unresolved matrix to chlorite and prehnite; note shards (arrows) and plagioclase pyroclasts (lower right corner); plane-polarized light photomicrograph of sample 71; scale bar = 0.05 mm.*

although its identification is complicated by considerable deformation. It is probable that a substantial proportion of vitric material has been dissolved during metamorphism- and deformation-related pressure solution (cf. Dimroth and Demarke, 1978).

Detrital Components of Sandstones (Connecting Point Group)

Lithic fragments

Rhyolite–dacite. Felsic volcaniclastic detritus in the entire sequence studied (Figure 2) is mostly of reworked, intrabasinal pyroclastic[1] origin, namely lithic and crystal tuff. Both pyroclastic and epiclastic fragments of cryptocrystalline quartz, and a mixture of quartz and feldspar, form the rhyolite–dacite lithic component of the sand fraction (Plates 2 and 3). Locally, clasts having quartz and plagioclase phenocryst, flow banding and fragments of spherulites, indicate that the observed 'chert-like' grains are fragments of aphanitic volcanic groundmass. The groundmass is dominated by cryptocrystalline, commonly spherulitic silica (Plate 2), which is locally recrystallised to mega-quartz, but also includes some K-feldspar. Idiomorphic areas are either irregular or linear, the latter defining flow banding.

Felsic volcanic sand grains in coarse-grained sandstones and conglomerates characteristically show porphyritic and glomeroporphyritic textures. Phenocrysts of quartz, up to 4 mm in size, are euhedral, embayed or considerably corroded having round outlines (Plate 2). Locally, biotite occurs as an accessory mineral.

Rare vesicular lithic particles have amygdules of quartz, chlorite, epidote and sphene. Felsic fragments exhibiting perlitic cracks occur in one sandstone sample (sample 26, Figure 2; Plate 4).

Andesite. Andesitic detritus is represented by a mixture of angular to well-rounded clasts of pyroclastic and epiclastic origin, ranging in size from sand to cobbles. It occurs throughout the entire succession of the Connecting Point Group, but conspicuously dominates the lithic fragments in the mixtite, as well as the deposits just below it, and also for 1500 m above it (Figure 2; Table 1).

Andesitic clasts are commonly porphyritic and glomeroporphyritic (Plate 5) containing embayed plagioclase and rarely augite phenocrysts (Plate 6) up to 1.2 mm long.

Plate 2. *A cobble-size epiclast of probable rhyodacitic composition; note the embayed quartz and feldspar phenocrysts and the spherulitic groundmass; cross-polarized light photomicrograph; scale bar = 0.25 mm.*

The andesitic fragments range from holocrystalline to hypocrystalline in which the glass is replaced mostly by chlorite, often in association with subordinate sphene and epidote. Quartz, feldspar (albite?), calcite and prehnite occur as less common forms of glass alteration. Apart from devitrified glass, hypocrystalline andesitic clasts are characterized by vesicles and skeletal plagioclase (Plates 5, 7 and 8), arranged in trachytic and variolitic textures. Trachytic and variolitic textures are also common in holocrystalline andesitic grains.

[1] In this report, the following definitions are adopted: **pyroclasts** are particles expelled through volcanic vents without reference to the causes of eruption or origin of the particles; **epiclasts** are produced by weathering and erosion of the volcanic rocks. Reworking and recycling of unconsolidated pyroclastic debris by water or wind *does not* transform pyroclasts into epiclastic fragments (see Fisher and Schmincke, 1984, p. 89.).

Plate 3. *Well rounded felsic epiclast surrounded predominantly by pyroclastic grains; arrows point to pumice fragments and shards; cross-polarized light photomicrograph of sample 72; scale bar = 0.25 mm.*

Pumice fragments (Plates 8 and 9) include hyaline types that appear to form a gradation of vesicular varieties derived from hypocrystalline andesite. Pumice fragments have irregular, jagged to multi-lobate shapes characteristic of lapilli (Plates 9 and 10). A subordinate proportion of rounded pumice fragments also occur. Ovoid to spherical vesicles are mostly filled with chlorite spherulites, commonly in association with quartz, feldspar and sphene. Calcite, clinozoisite and prehnite are less common in the amygdules. Shards of equivalent intermediate glass are rare, probably because they are less resistant to alteration compared to silicic glass (Fisher and Schmincke, 1984).

Schists. Schist fragments, as distinct from foliated volcanic tuff and groundmass altered to fine white mica and chlorite, occur in minor or trace amounts in the sand fraction throughout the studied sequence. Schist fragments, which are most abundant in a tuffaceous sandstone (sample 17, Figure 2 and Table 1; Plate 11), are represented by aggregates of muscovite ± biotite ± quartz ± garnet ± chlorite. Trace fragments of epidote-bearing siliceous schist have been identified in sample 54.

Intrusive rocks. Fragments of diorite (Plate 12) and microdiorite are a minor or trace constituent in the andesite-rich part of the succession. Microdiorite fragments are also

Plate 4. *Perlitic cracks in felsic sand grain; plane-polarized light photomicrograph of sample 63; scale bar = 0.05 mm.*

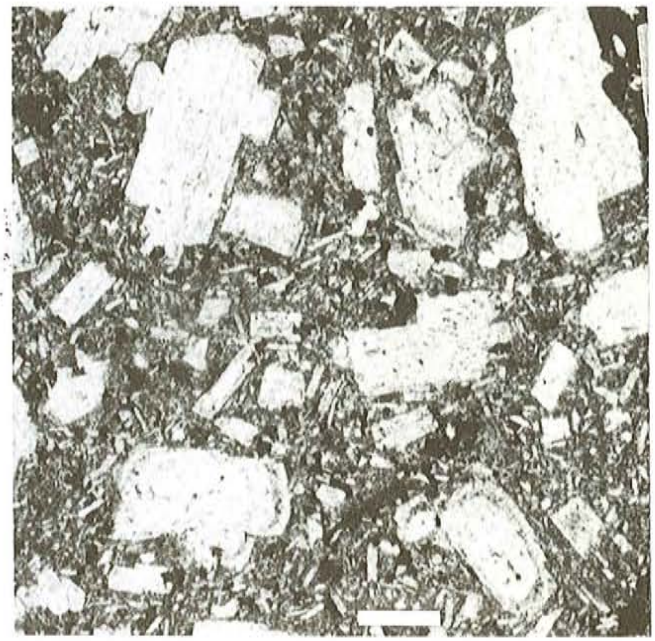

Plate 5. *Fragment of porphyritic andesite; large plagioclase phenocrysts showing zoning are embedded in a matrix of skeletal plagioclase crystals and cryptocrystalline groundmass that has been altered mainly to chlorite; plane-polarized light photomicrograph of sample 68; scale bar = 0.25 mm.*

Table 1: Mineralogy of detrital constituents in the deposits of the Love Cove Group (samples 1-8 and 30-34), and Connecting Point Group (the remaining samples)

Sample	1	2	3	4	5	6	7	8	9	10	11	12	13	14	15	16	17	18	19	20
Quartz (monocrystalline)	22.0	.	.	33.7	-	.	6.3	22.7	25.1	3.3	29.0	23.8	30.5	.	.	-	20.0	.	26.3	16.8
Quartz (polycrystalline)	12.7	.	.	20.3	-	-	2.0	13.3	5.0	1.3	8.9	11.4	5.7	.	.	-	6.0	.	9.3	15.0
K-feldspar	1.0	-	.	6.3	-	-	1.3	6.3	2.3	-	5.3	1.7	6.5	-	-	-	3.0	-	8.7	1.5
Plagioclase	9.3	.	.	3.6	-	.	82.3	10.0	28.4	93.7	13.6	27.5	6.5	.	.	-	6.0	.	13.7	1.8
Lithic fragments																				
Andesite	-	?	.	-	.	-	1.7	0.3	3.6	-	1.4	1.0	-	.	.	-	1.0	.	-	1.5
Rhyolite–dacite	43.7	?	.	27.3	.	.	5.7	42.7	31.1	-	32.9	24.2	37.0	.	.	.	50.5	.	34.0	42.5
Shards–pumice	-	.	-	-	-	-	-	-	-	-	-	3.3	-	-	-	-	-	.	tr	-
Tuff–tuffite	-	-	-	-	-	-	-	-	-	-	tr	tr	-	-	-	-	-	-	-	tr
Schist	1.0	-	-	0.6	.	-	-	1.7	-	-	-	0.7	-	-	-	.	8.5	.	-	tr
Other lithic fragments	4.3	-	-	[2,1]7.7	-	-	[3]tr	3.0	[1]3.3	[3]1.6	[1]8.2	10.5	-	[3]	-	3.5	7.3	[3,2]17.1	-	[3,2]17.1
Accessory minerals																				
Zircon	tr	-	-	-	-	-	-	tr	-	tr	tr	-	tr	-	.	-	tr	-	-	tr
Sphene	tr	-	-	-	-	-	-	-	tr	-	-	tr	-	-	-	-	-	-	tr	tr
Garnet	tr	-	-	tr	-	-	tr	tr	tr	tr	tr	-	tr	.	.	-	tr	.	tr	tr
Epidote	tr	-	-	-	-	-	-	-	-	-	tr	tr	tr	-	-	-	tr	-	-	tr
Allanite	-	-	-	-	-	-	-	-	-	-	-	tr	-	-	-	-	-	.	-	-
Tourmaline	-	-	-	-	-	-	-	-	tr	-	-	-	-	-	-	-	-	-	-	-
Clinopyroxene	-	-	-	tr	-	-	-	-	-	-	-	tr	-	-	-	-	-	-	tr	-
Orthopyroxene	tr	-	-	-	-	-	-	-	-	-	-	-	-	-	-	-	-	-	-	-
Muscovite	-	-	-	-	-	-	-	-	-	-	-	tr	-	-	-	-	-	-	tr	-
Biotite	-	-	-	.	-	-	-	-	tr	-	tr	tr	-	-	-	-	1.0	-	-	-
Chlorite	-	-	-	-	-	-	-	-	-	-	-	-	-	-	-	-	-	-	tr	-
Ore	2.3	-	-	-	-	-	-	-	-	-	-	0.7	-	-	-	-	-	-	-	-
Apatite	0.6	-	-	-	-	-	-	tr	tr	-	tr	-	tr	.	-	-	tr	.	tr	0.9
Matrix of the whole rock	76.4	X	X	X	X	X	44.9	67.0	81.5	39.0	86.6	80.6	83.8	X	X	X	83.5	X	79.7	69.7
Approximate grain size	cg	tuff cgl	cgl	mg	cgl	mg	cg	mg	cg	cg	cg	cg	fg	cgl	cgl	cgl	fg	mg	mg	cg

present; - absent; *–undifferentiated volcanic fragments; ?–identification uncertain due to recrystallization and deformation; X–not established; tr–trace; fg–fine-grained sandstone(ss.); mg–medium-grained ss.; cg–coarse-grained ss.; cgl–conglomerate; [1]–granite; [2]–undifferentiated intrusive rocks; [3]–microdiorite/diorite; [4]–trachyte; [5]–quartz arenite; [6]–quartzite.

Table 1: *(Continued)*

Sample	21	22	23	24	25	26	27	28	29	30	31	32	33	34	35	36	37	38	39	40	41	42
Quartz (monocrystalline)	10.5	.	13.0	5.3	11.3	17.0	11.7	.	16.7	.	.	.	.	.	.	.	.	.	.	.	.	.
Quartz (polycrystalline)	5.5	.	5.3	6.7	10.7	7.3	1.7	-	3.0	.	-	-	-	-	.	.	.	.	.	.	.	.
K-feldspar	2.0	-	3.3	1.0	4.3	3.7	1.0	-	-	-	-	.	-	-	.	.	.	.	-	-	.	.
Plagioclase	7.5	.	33.3	3.0	14.3	31.7	36.3	.	33.7	.	.	.	-	-	.	.	.	.	.	.	.	.
Lithic fragments																						
Andesite	-	-	7.0	-	4.7	7.0	7.3	.	8.7	.	.	-	-	-	.	-	.	.	.	.	-	-
Rhyolite–dacite	74.5	.	18.3	76.7	40.0	18.0	38.3	.	34.7	.	.	?	.	.	.	.	.	.	.	.	.	.
Shards–pumice	-	.	-	-	-	-	-	.	-	-	.	?	-	-	-	-	-	-	-	-	.	-
Tuff–tuffite	-	.	-	-	-	-	-	.	-	-	.	-	-	-	-	-	-	-	-	.	-	-
Schist	-	.	5.0	1.0	5.0	-	-	-	-		-	-	-	.	.	.	-	.	.	-	-	-
Other lithic fragments	-	-	12.3	5.0	7.8	[3]15.0	[3]2.7	[4]	2.3	-	[6]	-	-	-	[1]		[1]	-	[2]	-	-	-
Accessory minerals																						
Zircon	-	-	tr	-	tr	tr	-	-	tr	.	-	.	-	-	-	.	-	.	.	-	.	.
Sphene	-	.	-	-	-	tr	-	-	tr	-	-	-	-	-	.	-	-	-	-	-	-	-
Garnet	-	-	tr	tr	tr	tr	tr	-	tr	.	.	-	-	-	.	.	-	.	.	.	.	-
Epidote	-	-	tr	-	tr	-	-	-	-	-	.	-	-	-	.	.	-	-	-	-	-	-
Allanite	-	-	tr	-	tr	-	-	-	tr	-	-	-	-	-	-	-	-	-	-	-	-	.
Tourmaline	-	-	-	-	tr	-	-	-	-	-	-	-	-	-	-	-	-	-	-	-	.	-
Clinopyroxene	-	-	-	-	-	-	-	-	-	-	-	-	-	-	-	-	-	-	-	-	-	-
Orthopyroxene	-	-	-	-	-	-	-	-	-	-	-	-	-	-	-	-	-	-	-	-	-	-
Muscovite	-	-	tr	-	-	-	-	-	tr	-	-	-	-	-	-	-	-	-	-	.	-	-
Biotite	-	-	-	tr	tr	-	-	-	-	-	-	-	-	-	.	-	-	-	-	-	-	-
Chlorite	-	-	-	-	-	-	-	-	-	-	-	-	-	-	-	-	-	-	-	-	-	-
Ore	-	-	tr	-	-	-	-	-	-	-	-	-	-	-	-	-	-	-	-	-	-	-
Apatite	-	-	tr	tr	tr	tr	tr	-	tr	.	-	-	-	-	.	.	-	.	-	.	.	.
Matrix of the whole rock	5.6	X	48.9	44.0	66.3	47.7	24.8	X	50.1	X	X	X	X	X	X	X	X	X	X	X	X	X
Approximate grain size	cgl	cg	cg	cg	mg	cgl	cg	cgl	cgl	cgl	cgl	cgl	cgl	cgl	fg	mg	cg	cg	cgl	cgl	mg	cg

. present; - absent; *–undifferentiated volcanic fragments; ?–identification uncertain due to recrystallization and deformation; X–not established; tr–trace; fg–fine-grained sandstone(ss.); mg–medium-grained ss.; cg–coarse-grained ss.; cgl–conglomerate; [1]–granite; [2]–undifferentiated intrusive rocks; [3]–microdiorite/diorite; [4]–trachyte; [5]–quartz arenite; [6]–quartzite.

Table 1: *(Continued)*

Sample	43	44	45	46	47	48	49	50	51	52	53	54	55	56	57	58	59	60	61	62
Quartz (monocrystalline)		.	.	.	.	.	.	.	23.3	.	.	2.0	.	-	6.7	.	20.7	.	0.6	5.7
Quartz (polycrystalline)	.	.	.	.	.	.	.	-	5.0	-	-	-	-	-	-	.	-	-	-	-
K-feldspar	.	.	.	-	-	.	.	-	tr	.	-	-	-	-	0.7	-	-	-	-	-
Plagioclase	.	.	.	.	.	.	.	.	37.0	.	.	12.7	-	-	9.7	-	42.0	.	36.3	55.7
Lithic fragments																				
Andesite	-	-	.	-	-	-	-	-	1.0	.	-	3.3	.	.	12.0	.	7.0	.	44.3	29.0
Rhyolite–dacite	.	.	.	.	.	.	.	.	29.7	.	.	23.1	.	.	23.4	.	20.7	.	10.3	3.3
Shards–pumice	-	.	-	-	-	-	-	-	-	-	-	tr	-	.	-	-	-	-	6.0	0.6
Tuff–tuffite	.	.	.	-	-	-	-	-	-	-	.	49.0	.	.	38.1	.	7.7	-	-	-
Schist	-	.	-	-	-	-	-	-	1.0	-	-	4.3	-	.	-	-	-	.	-	
Other lithic fragments	-	.	[4]	-	[2]	[3,1]	-	-	3.0	-	[1,5,6]	4.7	[5,3]	[3,5,6]	9.4	[1,3]	2.0	-	2.0*	5.7*
Accessory minerals																				
Zircon	.	.	.	-	.	.	-	.	tr	.	.	-	.	-	-	.	-	.	-	-
Sphene	-	.	-	-	-	-	-	-	tr	.	-	-	-	-	-	-	tr	-	tr	-
Garnet	-	.	-	.	.	-	-	.	tr	-	-	tr	.	-	tr	-	tr	.	-	tr
Epidote	-	.	-	-	-	-	-	-	tr	-	-	-	-	-	-	-	tr	-	tr	tr
Allanite	-	.	.	-	.	-	-	-	-	-	-	-	-	-	-	-	-	-	-	-
Tourmaline	-	-	-	-	-	-	-	-	-	-	-	-	-	-	-	-	-	-	-	-
Clinopyroxene	-	-	-	-	-	-	-	-	-	-	-	-	-	-	-	-	-	-	tr	-
Orthopyroxene	-	-	-	-	-	-	-	-	-	-	-	-	-	-	-	-	-	-	-	-
Muscovite	.	-	-	-	-	-	-	-	-	.	.	-	.	-	-	.	-	-	-	-
Biotite	-	-	-	-	-	-	-	-	-	-	-	-	-	-	-	.	-	.	-	-
Chlorite	-	-	-	-	-	-	-	-	-	-	-	-	-	-	-	-	-	-	-	-
Ore	-	-	-	-	-	-	-	-	-	-	-	-	-	-	-	-	-	-	-	-
Apatite	.	.	-	-	.	-	-	.	-	-	-	-	-	-	-	-	-	-	-	-
Matrix of the whole rock	X	X	X	X	X	X	X	X	29.2	X	X	X	X	X	X	X	34.8	X	X	X
Approximate grain size	cg	cg	cg	mg	fg	cgl	mg	fg	cg	cg	cgl	cgl	cgl sl	cgl	cgl	cg	cgl	cg	cgl	mg

. present; - absent; *–undifferentiated volcanic fragments; ?–identification uncertain due to recrystallization and deformation; X–not established; tr–trace; fg–fine-grained sandstone(ss.); mg–medium-grained ss.; cg–coarse-grained ss.; cgl–conglomerate; [1]–granite; [2]–undifferentiated intrusive rocks; [3]–microdiorite/diorite; [4]–trachyte; [5]–quartz arenite; [6]–quartzite.

Table 1: *(Continued)*

Sample	63	64	65	66	67	68	69	70	71	72	73	74	75	76	77	78	79	80	81
Quartz (monocrystalline)	0.3	.	.	.	-	.	.	17.3	1.5	2.3	4.3	.	3.5	.	.	.	9.3	8.0	0.7
Quartz (polycrystalline)	-	-	-	.	-	-	-	-	-	-	-	-	-	-	-	-	-	-	-
K-feldspar	-	-	-	-	-	-	-	-	-	-	-	-	-	-	-	.	-	-	-
Plagioclase	34.0	.	.	.	.	.	-	41.0	37.0	35.0	24.3	.	39.0	.	.	-	41.3	54.0	52.0
Lithic fragments																			
Andesite	20.3	.	.	.	.	.	.	14.0	-	23.0	27.0	.	-	.	.	.	23.0	16.3	30.7
Rhyolite–dacite	8.7	-	.	.	.	.	.	26.7	1.0	9.0	9.0	.	3.0	.	.	.	13.3	15.3	10.7
Shards–pumice	2.3	-	-	-	-	.	-	-	60.5	13.0	7.7	-	53.5	.	-	-	7.7	tr	-
Tuff–tuffite	14.0	-	-	-	-	.	-	-	-	13.3	22.0	-	-	-	.	.	2.0	-	4.0
Schist	-	-	-	-	-	.	-	-	-	-	-	-	-	-	-	.	-	-	-
Other lithic fragments	11.3*	[5]	-	-	-	[3]	[3]	1.0*	-	4.3*	5.7*	-	-	[6]	-	-	3.3*	6.3*	2.0*
Accessory minerals																			
Zircon	-	.	-	-	-	.	.	-	-	-	tr	.	-	-	.	-	-	-	-
Sphene	-	-	-	-	-	-	-	-	-	-	-	-	-	-	-	-	-	-	-
Garnet	tr	-	-	.	-	-	.	-	-	-	tr	.	-	-	.	.	-	-	-
Epidote	-	-	-	-	-	-	-	tr	-	-	tr	-	-	-	-	-	-	-	-
Allanite	-	-	-	-	-	-	-	-	-	-	-	-	-	-	-	-	-	-	-
Tourmaline	-	-	-	-	-	-	-	-	-	-	-	-	-	-	-	-	-	-	-
Clinopyroxene	-	-	-	-	-	-	-	tr	-	tr	-	-	-	-	-	-	-	tr	-
Orthopyroxene	-	-	-	-	-	-	-	-	-	-	-	-	-	-	-	-	-	-	-
Muscovite	-	-	-	-	-	-	-	-	-	-	-	-	-	-	-	-	-	-	-
Biotite	-	-	-	-	-	-	-	-	-	-	-	-	-	-	-	-	-	tr	-
Chlorite	-	-	-	-	-	-	-	-	-	-	-	-	-	-	-	-	-	-	-
Ore	-	-	-	-	-	-	-	-	-	-	-	-	-	-	-	-	-	-	-
Apatite	-	-	.	-	-	.	-	-	1.0	-	-	.	-	-	-	-	.	-	-
Matrix of the whole rock	X	X	X	X	X	X	X	X	86.0	X	80.4	X	89.6	X	X	X	X	X	X
Approximate grain size	cgl	mg	cgl	fg	cgl	cgl	cgl	cgl	tuff mg	cgl	cgl	cg	tuff mg	mg	mg	cg	cg	cg	cgl

. present; - absent; *–undifferentiated volcanic fragments; ?–identification uncertain due to recrystallization and deformation; X–not established; tr–trace; fg–fine-grained sandstone(ss.); mg–medium-grained ss.; cg–coarse-grained ss.; cgl–conglomerate; [1]–granite; [2]–undifferentiated intrusive rocks; [3]–microdiorite/diorite; [4]–trachyte; [5]–quartz arenite; [6]–quartzite.

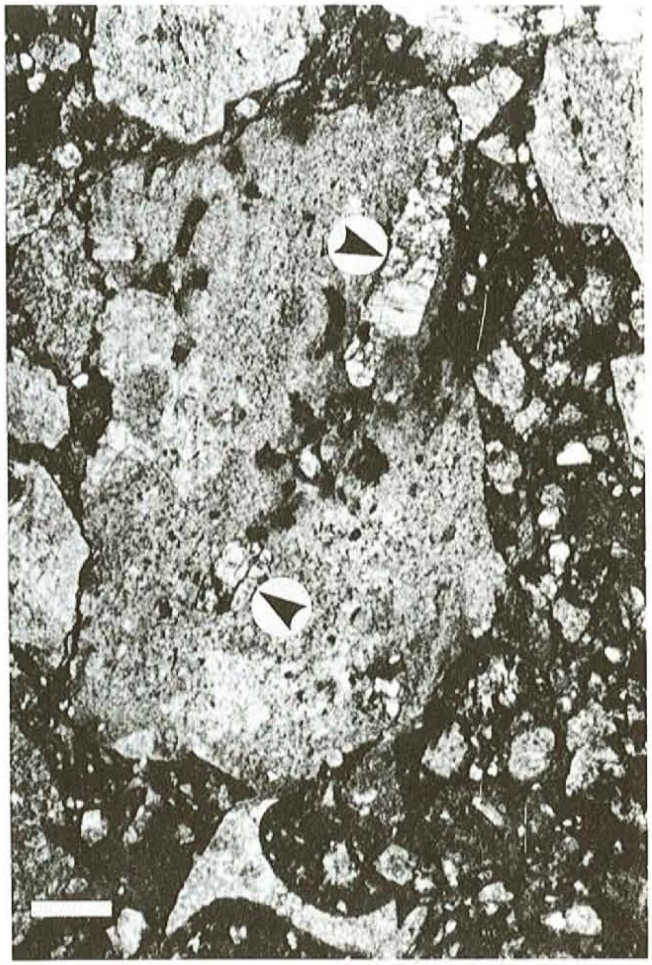

Plate 6. *Andesitic fragment containing augite phenocrysts (arrowed); note T-shaped felsic shard; plane-polarized light photomicrograph of sample 61; scale bar = 0.25 mm.*

Plate 7. *Vesicular pyroclast pebble containing skeletal plagioclase crystals; the vesicles are filled with chlorite; plane-polarized light photomicrograph of sample 72; scale bar = 0.05 mm.*

present in anomalous arkosic sandstone samples 7 and 10 (Figure 2), which consist dominantly of plagioclase feldspar and the occasional garnet inclusions; clasts of medium- to fine-grained granite are uncommon.

Sedimentary rocks. Angular fragments of intrabasinal tuff, tuffaceous sandstone and siltstone, occur in variable (usually trace) amounts in the deposits of the Connecting Point Group. In samples 54, 57, 63, 72 and 73 they are particularly abundant (Table 1; see also Plates 12 and 13 in Knight and O'Brien, 1988). There is also a minor proportion of well-rounded tuff and tuffaceous fragments, which may represent an extrabasinal component. Rare extrabasinal fragments of quartz arenite occur locally (Plates 12 and 13).

Dētrital mineral grains

Quartz. Detrital quartz is present as mono- and polycrystalline grains, ranging from angular and subangular to less commonly well rounded. Polycrystalline grains usually have polygonal intercrystalline boundaries. Rounded monocrystalline quartz is often embayed, suggesting that the roundness was caused by magmatic corrosion rather than being related to sediment transport. The quartz component in the sediments, clearly decreases upward through the succession (Figure 3).

Feldspar. Plagioclase in angular to subrounded grains is the dominant feldspar. Corrosion-rounded plagioclase phenocrysts in accompanying volcanic clasts suggest that the rounded plagioclase grains may have inherited their shape. Plagioclase grains are commonly replaced by albite and K-feldspar or altered to white mica, chlorite, calcite, sphene and epidote. Orthoclase (microperthites) and microcline occur locally.

Plagioclase-rich arkoses and feldspar, ranging from 82 to 93 percent of the sand fraction, are represented by two samples (samples 7 and 10) in the Love Cove Group and lowest unit (C-1; Figure 2) of the Connecting Point Group. Both occur in facies H sandstones of Knight and O'Brien (1988).

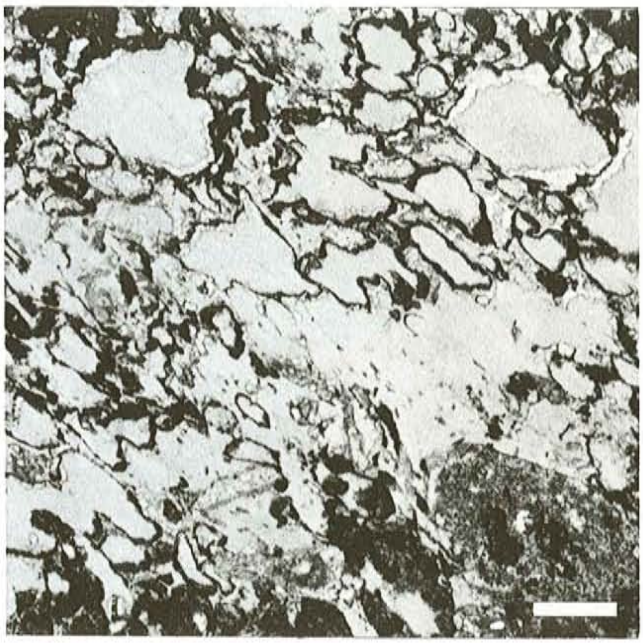

Plate 8. *Pumice fragment of andesitic-basaltic composition. Glass has mainly been replaced by chlorite. Secondary quartz, epidote and sphene are also present. The fine-grained, granular sphene outlines the margins of the vesicles. Bedding is inclined at an angle of around 30° to the right; plane-polarized light photomicrograph of sample 2; scale bar = 0.05 mm.*

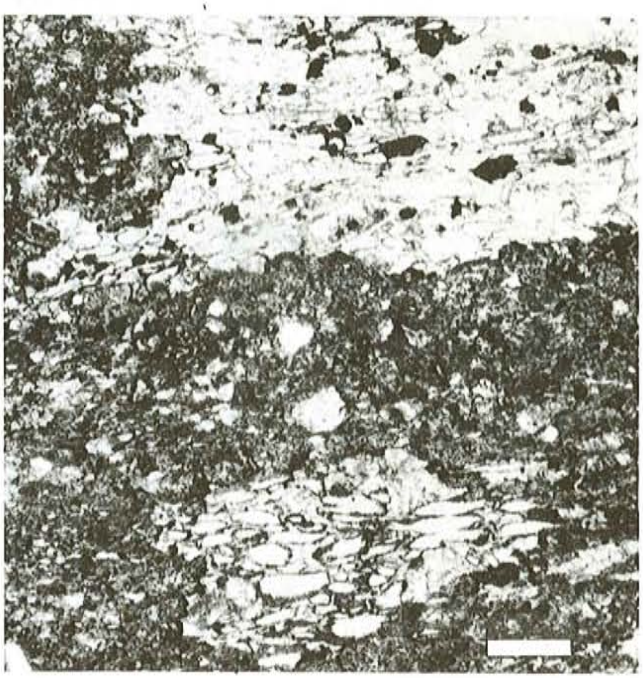

Plate 9. *Jagged pumice fragments showing bedding-parallel flattening; because some of the pumice particles experienced very little deformation, it is inferred that tectonic origin of this texture is unlikely; plane-polarized light photomicrograph of sample 2; scale bar = 0.25 mm.*

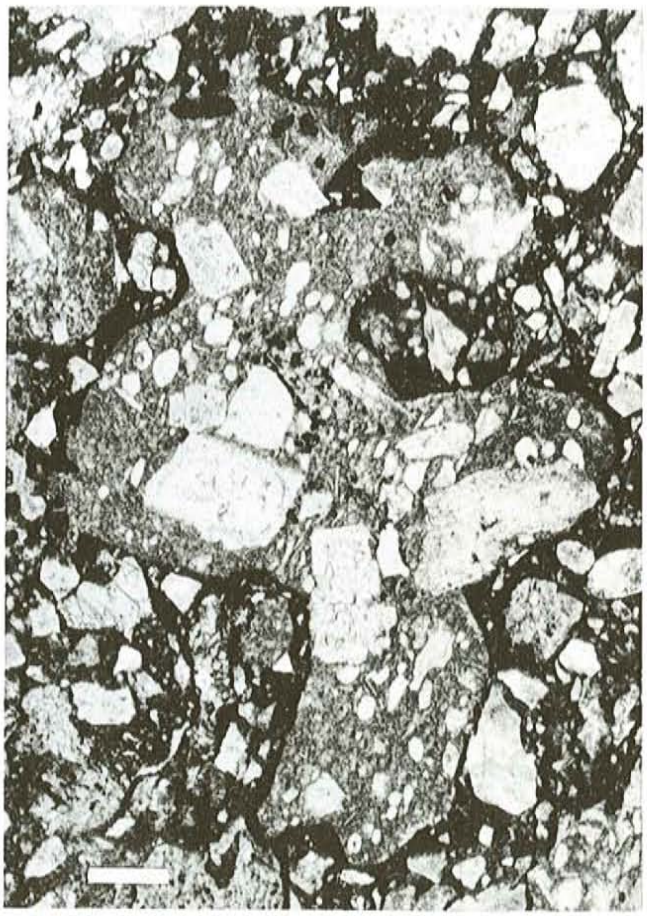

Plate 10. *Multi-lobate, andesitic lapilli; the vesicles are mostly filled with chlorite and plagioclase phenocrysts are overgrown by albite(?); plane-polarized light photomicrograph of sample 61; scale bar = 0.25 mm.*

Accessory mineral grains. Garnet is the most common accessory mineral and occurs as euhedral, round and angular grains, ranging in size from 0.01 to 0.12 mm (Plate 14). Garnet has been found associated with muscovite–biotite schist fragments. Small garnet inclusions occasionally also occur in plagioclase crystals associated with the intermediate volcanic and intrusive lithic fragments. Zircon, apatite and allanite are less common; their average size is 0.05, 0.08 and 0.16 mm respectively. Sphene, epidote, opaque minerals (principally pyrite), and magnetite are also present, but it is very often impossible to draw a distinction between the detrital grains and the secondary crystals. Augite and tourmaline are the least common accessory minerals.

Matrix

The dominant component of most of the sediments in the Connecting Point Group is a ubiquitously altered, fine-grained matrix (<0.0626 mm). It comprises up to 86 percent of some samples (Table 1). Cryptocrystalline quartz, feldspar, sericite, muscovite, chlorite and calcite, commonly replace

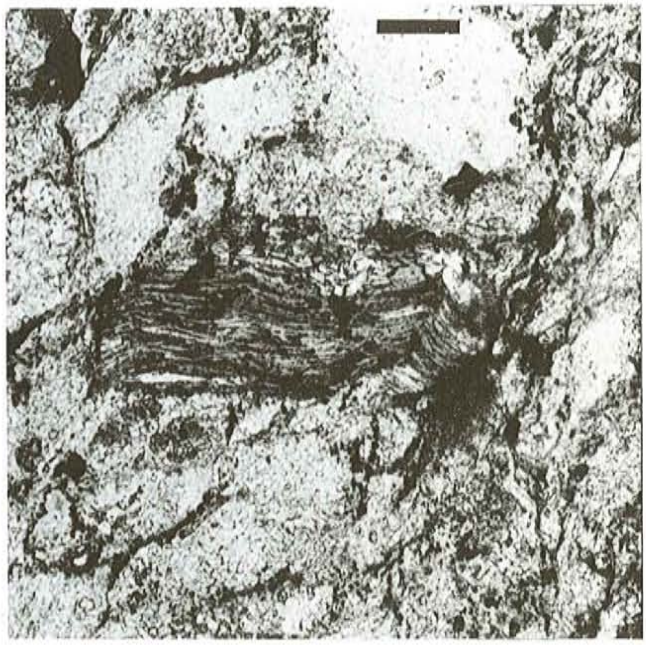

Plate 11. *Slightly deformed fragment of biotite–muscovite schist enclosed in devitrified tuffaceous matrix; plane-polarized light photomicrograph of sample 17; scale bar = 0.25 mm.*

the original matrix. Epidote, clinozoisite, sphene, prehnite and pyroxene are other, less common, secondary minerals. Relicts of shards and pumice occur locally and suggest that the matrix in the sandstones and conglomerates was originally felsic lithic and crystal tuff material.

Relationship Between Existing Lithostratigraphy and Petrography

The petrographic study generally confirms the lithostratigraphic correlations between sections of the Connecting Point Group, originally established by Knight and O'Brien (1988). It also identifies a compositional change of lithic clasts in the sandstones, from dominantly felsic below the mixtite, to andesite-dominant, at and for 1500 m above the mixtite (Figure 3).

The granule conglomerate from the Willis Reach section (sample 59, Figure 2) has a different composition from the other samples of the granule conglomerate (Table 1), collected from the mixtite horizon, with which it is correlated. This disparity does not necessarily imply an incorrect correlation. It may merely reflect a compositionally heterogeneous nature of the mixtite sheet, which in turn reflects the lithological inhomogeneities of the source sediments, which were present along the slope of the Eastport basin, prior to the remobilisation and emplacement of the mixtite.

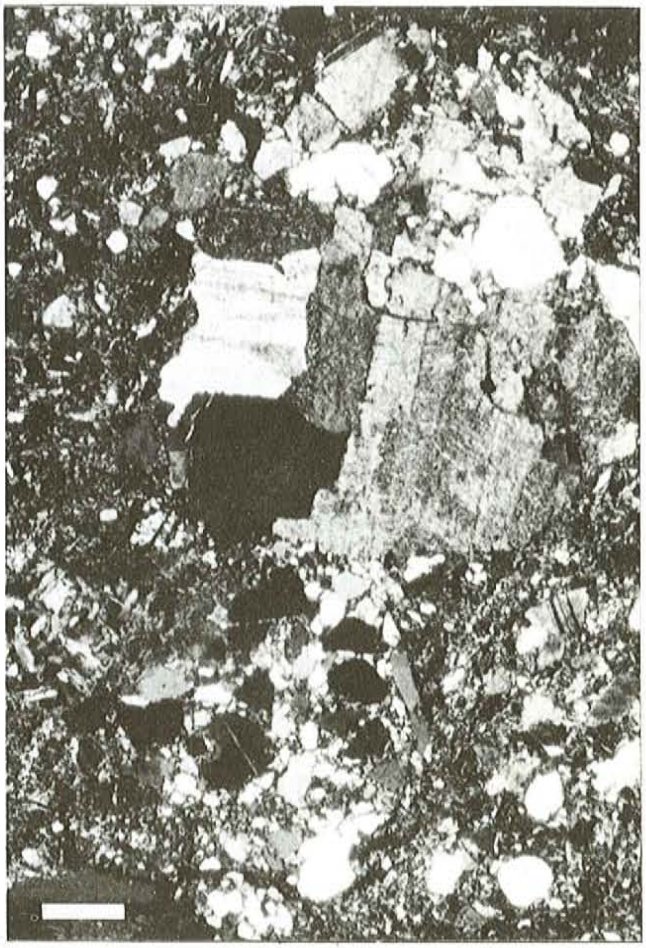

Plate 12. *Sand-size grains of microdiorite (above) and quartz arenite; cross-polarized light photomicrograph of sample 56; scale bar = 0.25 mm.*

Pyroclastic versus Epiclastic Origin

Petrographic textures and sedimentary structures indicate that most of the sediments in the Love Cove and Connecting Point groups were derived by reworking of dominantly pyroclastic deposits of a penecontemporaneous volcanic arc apron. Autochthonous tuffs in the Connecting Point Group (samples 71 and 75, Figure 2) show no petrographic evidence of welding. However, some of the deposits in the upper Love Cove Group and the lowest Connecting Point Group may have formed from pyroclastic surges (cf. Ayres, 1982). The existence of possible eutaxitic textures provide inconclusive evidence of welding in thin, fine-grained, glassy beds interpreted as tuffs by Knight and O'Brien (1988, facies B) (Plate 9).

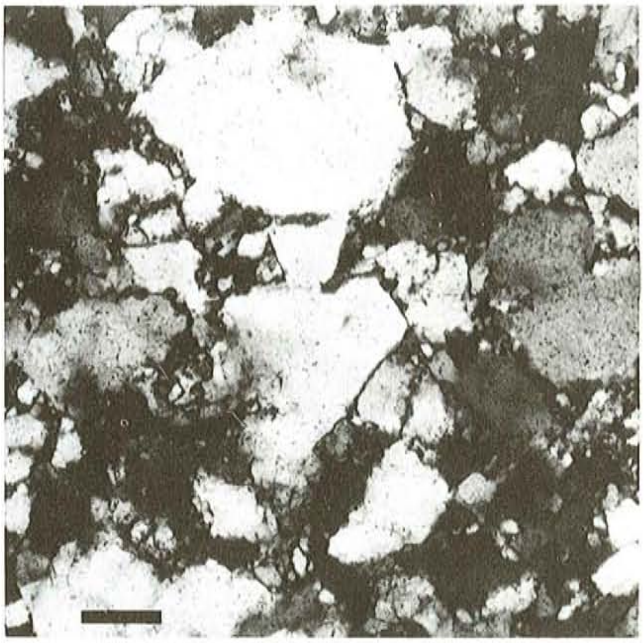

Plate 13. *Sand grain of quartz arenite; cross-polarized light photomicrograph of sample 56; scale bar = 0.05 mm.*

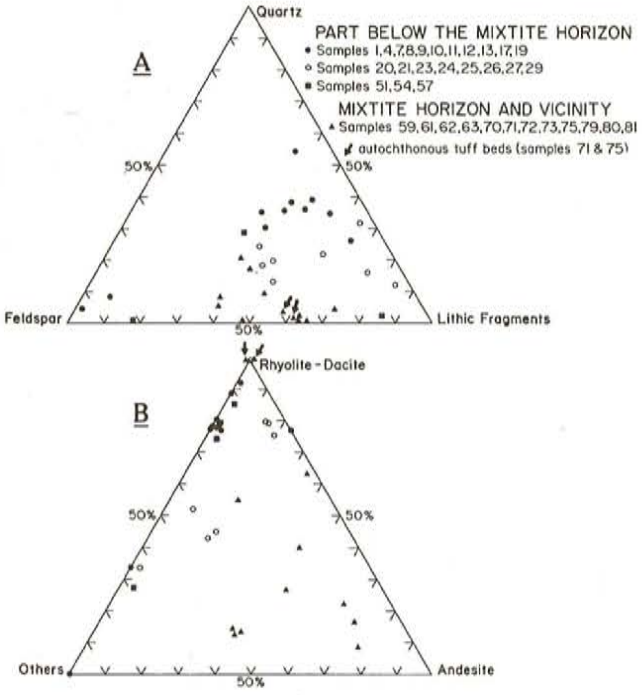

Figure 3. *(A) Standard trigonal diagram summarizing petrographic composition of the detrital fraction in the upper part of the Love Cove Group and the overlying Connecting Point Group. The diagram illustrates an upward decrease of the quartz component (''immaturing-upwards''); (B): discrimination of lithic fragments in the same samples as in A shows an increase in proportion of andesitic detritus at the mixtite horizon.*

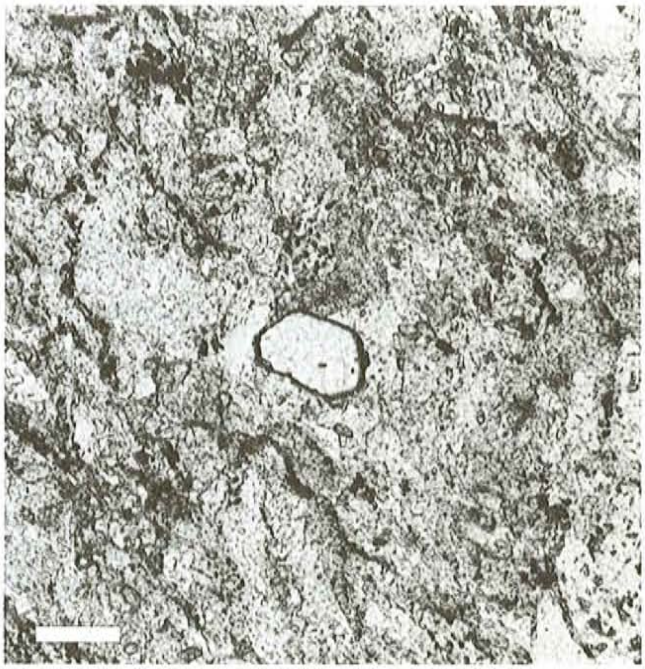

Plate 14. *Euhedral grain of garnet set in devitrified tuffaceous matrix; garnet also appears as a constituent of biotite–muscovite schist fragments; plane-polarized light photomicrograph of sample 17; scale bar = 0.25 mm.*

Provenance of the Sediments of the Love Cove and Connecting Point Groups

Felsic pyroclastic material, represented by a fine-grained matrix and rhyolitic–dacitic lithoclasts, predominate the entire upper part of the Love Cove Group, and the overlying Connecting Point Group. It records a period of almost continuous felsic pyroclastic volcanism, which released vast volumes of ash into the adjacent Eastport basin. Although a few autochthonous crystal tuff beds have been examined from both below and above the mixtite horizon, (samples 71 and 75, Figure 2), most of the fallout tephra underwent remobilisation prior to final deposition on the submarine apron (Knight and O'Brien, 1988). The resultant tuffaceous deposits are heterolithic and are enriched in the lithic volcanogenic material, as well as in quartz and plagioclase of both pyroclastic and epiclastic origin. This aspect of resedimentation is best demonstrated by the mixtite, which comprises large blocks of tuffite and volcanigenic conglomerate (Plates 12 and 13 in Knight and O'Brien, 1988), and where the matrix contains abundant vitric, felsic fragments (Table 1). The autochthonous tuff bed (sample 71, Figure 2), represents a possible source of the felsic vitric material, which is present in the mixtite directly above.

The upward decrease in the proportion of quartz may reflect a significant decline in, 1) the proportion of epiclastic detritus in the source area, and 2) the proportion of material

derived from erosion of basement rocks. This 'immaturing-upwards' may also reflect a decrease in the proportion of sediment that underwent textural modification in fluvial, deltaic or shallow marine settings prior to the resedimentation. This consequently implies an upward increase in the amount of pyroclastic detritus in the turbidites, and is supported by the conspicuously abundant tuffaceous material associated with the mixtite horizon, where it appears as both autochthonous tuff beds (samples 71 and 75, Figure 2), clasts (samples 69 and 70, Figure 2), and as matrix in the conglomerates (samples 72 and 73, Figure 2). This overall trend probably, partly reflects the generation of large quantities of pyroclastic material in the vicinity of the arc, overwhelming the basin processes and resulting in slope instabilities, which readily led to downslope remobilisation. In addition, it also may reflect the widening of the arc basin with time (Knight and O'Brien, 1988), explaining the upward change from a low-efficiency deep-water fan setting, to fans composed of well-developed channel and levée complexes. When the basin was narrow with steep sides, sediment reworked by nearshore and fluvial processes along the basin margins was readily moved basinward, down the slope. This scenerio is supported by mega-turbidites of plagioarkosic sandstones (see next section) that occur in this succession. As a result when the basin widened and slopes declined, these zones of shallow water sediment reworking would be effectively isolated by the apron from the basin depocenter, so that progressively, less reworked detritus was remobilised and transported basinward.

Andesitic and associated dioritic detritus is most conspicuous in the mixtite horizon and the deposits above it. Andesite fragments range from vitric to lithic, and their variable roundness may indicate that they are a mixture of epiclastic and pyroclastic material. This sudden increase in the proportion of the andesitic detritus suggests a change in the composition of volcanism in the vicinity of the Eastport basin. It appears to have coincided with an episode of basin extension and accompanying mafic intrusions (Knight and O'Brien, 1988). The andesitic material is accompanied by pyro- and epiclastic rhyolite–dacite detritus showing that felsic volcanism, although less important, was almost continuously active during the sedimentation of the Connecting Point Group.

As is the case of most resedimented volcaniclastic rocks, (e.g., Schmincke and von Rad, 1979; Fisher and Schmincke, 1984; Cas and Wright, 1988) the Connecting Point Group contains various amounts of non-volcanic components. Fragments of intrusive, metamorphic and clastic sedimentary rocks were incorporated during the formation of the tuffaceous turbidites, the debris flow conglomerates and the olistostrome deposits. Generally, the metamorphic detritus appears in trace amounts; however, in the tuffite (sample 17, Figure 2), sand-size schist fragments are exceptionally abundant (8.5 percent). The enrichment might have occurred through winnowing of the vitric material and/or by incorporation of new detritus.

The origin of these metamorphic, dioritic, granitic and quartz arenite fragments is uncertain. They are either, 1) accidental constituents captured from an eruptive vent during an explosive eruption (Fisher and Schmincke, 1984; Suzuki-Kamata, 1988), or 2) the product of erosion of exposed areas of continental crust and/or island-arc crust.

Sedimentary rock fragments are predominantly represented by intrabasinal tuff and tuffaceous rock fragments (see also Plates 12 and 13 in Knight and O'Brien, 1988).

Compositionally Distinct Sandstones

Petrographically and texturally distinct arkosic sandstones occur in two units of graded, planar-stratified sandstones (facies H, Knight and O'Brien, 1988), in the first 800 m of the section on Long Reach Island (samples 7 and 10, Figure 2). Throughout the section other units of this facies have a mineralogy similar to the rest of the sequence. The arkoses are well sorted with angular to subrounded grains and contain lithic grains of microdiorite. The facies units have restricted lateral distribution in the fine grained, basinal and distal fan deposits. Locally, they fill channels within levée deposits. The two examples described, occur within distal fan turbidites of the lower part of the succession that are compositionally lithic arenites and have a predominantly felsic component. This suggests that the arkose were derived from a distinct source, probably a pluton, and when transported as mega-turbidites, they were able to bypass the volcaniclastic apron, and not loose their mineralogical identity by dispersal in shallow- or deep-water settings. The source may have been a subvolcanic dioritic–microdioritic pluton, which was exposed and eroded by a single river that constructed a delta or shoreline sand body of distinct detrital composition. The sands were remobilised soon after and travelled as mega-turbidites to basinal depths.

Subaerial or Submarine Eruptions

The widespread presence of the felsic and intermediate epiclastic detritus in the succession of the Eastport basin and the local occurrence of reworked arkosic detritus (samples 7 and 10; Figure 2) indicate a subaerially exposed volcanic -intrusive edifice, as the source of a substantial proportion of the detritus released into the basin. The widely distributed but uncommon schist, granite and quartz arenite detritus additionally suggest an emergent terrane having a possible metamorphic basement to the volcanic-subvolcanic edifice.

Extensive pyroclastic volcanism is not likely to begin until a volcano is either above or close to sea level (Ayres, 1982). In particular, the subaerial parts of volcanoes of silicic to intermediate composition, are known to yield a great amount of the pyroclastic detritus (Fisher and Schmincke, 1984; Cas and Wright, 1988). An abundant supply of unconsolidated pyroclastic sediments is critical in explaining the abundance of the resedimented facies in the Eastport basin.

The vitric material recognized in the Connecting Point Group is characterised by a high degree of vesiculation and the andesitic lapilli commonly contain quench plagioclase, indicative of rapid cooling (Gelinas and Brooks, 1974). These features additionally support the subaerial and/or shallow-water nature of the felsic to intermediate volcanic eruptions (Heiken, 1972; Fisher and Schmincke, 1984). Hyaloclastic material, which is diagnostic of submarine eruptions (Fisher and Schmincke, 1984), has not been identified in the group.

Comments on Sedimentary Processes

A significant proportion of the detritus in the Connecting Point Group, probably underwent recycling in fluvial or shallow-marine settings prior to transportation onto the volcaniclastic apron. This is suggested by numerous well rounded clasts of various lithologies (Plate 2) and locally by good sorting of the sand grains (sample 10; Figure 2). However, it is noteworthy that a significant degree of roundness can also be achieved during pyroclastic eruption because of the high concentration of pyroclasts passing through the eruptive vent (Cas and Wright, 1988).

In volcaniclastic sediments, the rate of glass divitrification is sufficiently rapid to produce a significant amount of smectite (Vessel and Davis, 1981; Fisher and Schmincke, 1984). It is inferred that the presence of this expandable clay in the sediments of the Eastport basin might have considerably increased the cohesion factor of the gravity flows during resedimentation and hence facilitated development of high-density turbidity currents. In addition, smectite-rich sediments, as well as ash-water mixtures, have thixotropic properties and, therefore, slopes composed of such sediments would be highly unstable and prone to collapse (e.g., Busby-Spera, 1988).

CONCLUSIONS

The results of this petrographic study strongly support the volcanic arc-related geotectonic setting of the Eastport basin and the sedimentation of the Connecting Point Group, proposed by Knight and O'Brien (1988). Penecontemporaneous volcanic rocks ranging from rhyolites to andesites suggest a mature island-arc complex with a substrate of continental and/or island-arc crust, including medium- to high-grade metamorphic rocks (cf. Hamilton, 1988) that supplied subordinate metamorphic, plutonic and quartz arenite detritus.

More field work is necessary in order to carry out clast counts in the mixtite horizon and the adjacent coarse-grained deposits. This would give a more precise estimate of the proportions of various lithic components present in the Connecting Point Group. Further detailed petrographic work and bulk geochemical analyses on the clasts will enable a better understanding of the volcanic source area and its comparison with volcanic rocks of the contemporaneous Love Cove Group. Collection of additional samples of sandstones from selected horizons will supplement and confirm the existing petrographic data of the Connecting Point Group. Microprobe analysis of detrital garnet, feldspars and pyroxene should help to better define composition and origin of source rocks in the volcanic arc and in its substrate.

REFERENCES

Ayres, L.D.
1982: Pyroclastic rocks in the geologic record. *In* Pyroclastic volcanism and deposits of Cenozoic intermediate to felsic volcanic islands with implications for Precambrian Greenstone-Belt volcanics. Geological Association of Canada, Short Course Notes, Volume 2, pages 1-17.

Busby-Spera, C.J.
1988: Development of fan-deltoid slope aprons in a convergent-margin tectonic setting: Mesozoic, Baja California, Mexico. *In* Fan Deltas: Sedimentology and Tectonic Settings. *Edited by* W. Nemec and R.J. Steel. Blackie and Son, Glasgow and London, 444 pages.

Cas, R.A.R. and Wright, J.Y.
1987: Volcanic successions, modern and ancient. A geological approach to processes, products and successions. Allen and Unwin, London, 528 pages.

Dickinson, W.R.
1970: Interpreting detrital modes of greywacke and arkose. Journal of Sedimentary Petrology, Volume 90, pages 695-707.

Dimroth, E. and Demarcke, J.
1978: Petrography and mechanism of eruption of the Archean Dalembert tuff, Rouyn–Noranda, Quebec, Canada. Canadian Journal of Earth Sciences, Volume 15, pages 1712-1723.

Fisher, R.Y. and Schmincke, H.-V.
1984: Pyroclastic Rocks. Springer-Verlag, Berlin, Heidelberg, New York, Tokyo, 472 pages.

Gélinas, L. and Brooks, C.
1974: Archean quench-texture tholeiites. Canadian Journal of Earth Sciences, Volume 11, pages 324-340.

Hamilton, W.B.
1988: Plate tectonics and island arcs. Geological Society of America Bulletin, Volume 100, pages 1503-1527.

Hayes, A.O.
1948: Geology of the area between Bonavista and Trinity Bays, eastern Newfoundland. Geological Survey of Newfoundland, Bulletin 32, Part 1, pages 1-34.

Heiken, G.H.
1972: Morphology and petrography of volcanic ashes. Geological Survey of America Bulletin, Volume 83, pages 1961-1988.

Ingersoll, R.V., Bullard, T.F., Ford, R.I., Grim, J.P., Pickle, J.D. and Sares, S.W.
1984: The effect of grain size on detrital modes: a test of the Gazzi-Dickinson point-counting method. Journal of Sedimentary Petrology, Volume 54, pages 103-116.

Knight, I. and O'Brien, S.J.
1988: Stratigraphic and sedimentological studies of the Connecting Point Group, portions of the Eastport (12C/12) and St. Brendan's (2C/13) map areas, Bonavista Bay, Newfoundand. *In* Current Research. Newfoundland Department of Mines, Mineral Development Division, Report 88-1, pages 207-227.

O'Brien, S.J.
1987: Geology of the Eastport (west half) map area. Bonavista Bay, Newfoundland. *In* Current Research. Newfoundland Department of Mines and Energy, Mineral Development Division, Report 87-1, pages 257-270.

O'Brien, S.J. and Knight, I.
1988: The Avalonian geology of southwest Bonavista Bay: portions of the St. Brendan's (2C/13) and Eastport (2C/12) map areas. *In* Current Research. Newfoundland Department of Mines, Mineral Development Division, Report 88-1, pages 193-205.

Schmincke, H.-U. and von Rad, V.
1979: Neogene evolution of Canary Island volcanism inferred from ash layers and volcaniclastic sandstones of DSDP site 397 (Leg 47A). *In* Initial Reports, Deep Sea Drilling Project 47, Part 1. *Edited by* V. von Rad, W.B.F. Ryan, *et al.* pages 703-725.

Schmincke, H.-U. and Swanson, D.L.
1967: Laminar viscous flowage structures in ash-flow tuffs from Gran Canaria, Canary Islands. Journal of Geology, Volume 76, pages 641-664.

Suzuki-Kamata, K.
1988: The ground layer of Ata pyroclastic flow deposit, southwestern Japan—evidence for the capture of lithic fragments. Bulletin of Volcanology, Volume 50, pages 119-129.

Vessel, R.K. and Davis, D.K.
1981: Non marine sedimentation in an active fore arc basin. SEPM Special Publication No. 31, pages 31-45.

Zuffa, G.G.
1980: Hybrid arenites: their composition and classification. Journal of Sedimentary Petrology, Volume 50, Number 1, pages 21-29.

1985: Optical analyses of arenites: influence of methodology on compositional results. *In* Provenance of Arenites. *Edited by* G.G. Zuffa. D Rendel Publishing Co., pages 165-189.